Soft x-ray emission spectroscopy studies of the electronic structure of silicon supersaturated with sulfur

J. T. Sullivan,[1,a)] R. G. Wilks,[2] M. T. Winkler,[1] L. Weinhardt,[3] D. Recht,[4] A. J. Said,[4] B. K. Newman,[1] Y. Zhang,[5] M. Blum,[5,6] S. Krause,[5] W. L. Yang,[6] C. Heske,[5] M. J. Aziz,[4] M. Bär,[2,7] and T. Buonassisi[1]

[1]*Department of Mechanical Engineering, Massachusetts Institute of Technology, Cambridge, Massachusetts 02139, USA*
[2]*Solar Energy Research, Helmholtz-Zentrum Berlin für Materialien und Energie GmbH, Lise-Meitner-Campus, Hahn-Meitner-Platz 1, 14109 Berlin, Germany*
[3]*Experimentelle Physik VII, Universität Würzburg, Am Hubland, 97074 Würzburg, Germany*
[4]*Harvard School of Engineering and Applied Sciences, Cambridge, Massachusetts 02138, USA*
[5]*Department of Chemistry, University of Nevada, Las Vegas, 4505 Maryland Pkwy, Las Vegas, Nevada 89154-4003, USA*
[6]*Advanced Light Source, Lawrence Berkeley National Laboratory, 1 Cyclotron Road, Berkeley, California 94720, USA*
[7]*Institut für Physik und Chemie, Brandenburgische Technische Universität Cottbus, Konrad-Wachsmann-Allee 1, 03046 Cottbus, Germany*

(Received 25 July 2011; accepted 26 August 2011; published online 3 October 2011)

We apply soft x-ray emission spectroscopy (XES) to measure the electronic structure of crystalline silicon supersaturated with sulfur (up to 0.7 at. %), a candidate intermediate-band solar cell material. Si $L_{2,3}$ emission features are observed above the conventional Si valence band maximum, with intensity scaling linearly with S concentration. The lineshape of the S-induced features change across the insulator-to-metal transition, indicating a significant modification of the local electronic structure concurrent with the change in macroscopic electronic behavior. The relationship between the Si $L_{2,3}$ XES spectral features and the anomalously high sub-band gap infrared absorption is discussed. © *2011 American Institute of Physics*. [doi:10.1063/1.3643050]

One intermediate band (IB) solar cell[1] absorber material is formed by introducing deep-level impurities at high concentration to form a mid-gap impurity band that facilitates the absorption of sub-bandgap photons while suppressing non-radiative recombination.[2] Si doped with S—a deep-level donor in Si (Ref. 3)—to above 0.7 at. % is a candidate IB photovoltaic absorber when partially compensated,[4] exhibiting strong sub-band gap absorption[5,6] and metallic conductivity[7] that suggest the formation of a deep-level dopant induced band. In this letter, we present Si $L_{2,3}$ x-ray emission spectra (XES) of crystalline Si doped with S that reflect the altered electronic structure.

Si supersaturated with S can be fabricated using laser incorporation of S-bearing gases[6] or ion-implantation followed by pulsed laser melting (PLM).[8] We use ion-implantation followed by PLM because it produces single-crystal[8–10] samples and provides accurate S concentration control. 700-μm thick, *p*-type Si wafers (10–20 Ω-cm, double-side polished, Czochralski-grown, (100) orientation) were ion-implanted at 95 keV with $^{32}S^{+}$ at 7° off-normal to prevent channeling. Four different wafers were implanted with S at doses of 3×10^{14}, 1×10^{15}, 3×10^{15}, and 1×10^{16} cm^{-2}, respectively. Implanted wafers were irradiated with four consecutive XeCl laser pulses (308 nm, 25 ns at full width at half maximum (FWHM), 50 ns total duration, fluences 1.7, 1.7, 1.7, and 1.8 J/cm^2). The beam was homogenized to <5% root-mean square intensity variation over a 2.5×2.5 mm^2 area. Following PLM, two samples with the highest (1×10^{16} cm^{-2}) S dose were annealed for 30 min in an N_2 atmosphere at 400 °C and 900 °C, respectively.

S concentrations measured[7] by secondary ion mass spectrometry (SIMS) for two samples implanted to doses of 3×10^{15} cm^{-2} and 1×10^{16} cm^{-2} yield peak concentrations of 1.2×10^{20} and 3.8×10^{20} cm^{-3}, respectively. SIMS measurements were largely unaffected by concentration-dependent ionic yields for sulfur because comparison of as-implanted profiles normalized to peak value were in good agreement (within 7% maximum error) for both samples. The SIMS data for the post-PLM samples were extrapolated linearly to estimate the peak S concentrations in the 3×10^{14} and 1×10^{15} cm^{-2} samples, which are 1.4×10^{19} and 4.0×10^{19} cm^{-3}, respectively. Over 95% of S-dopants are concentrated in a layer about 350 nm deep.

We refer to un-annealed samples by their peak S concentration (in S cm^{-3}) and to annealed samples by their annealing temperature. Errors on peak concentration are ±20%. A control sample from the same substrate—which was neither implanted nor laser-melted—is referred to as "Si reference."

For each sample, absorptance was measured using a spectrophotometer equipped with an integrating sphere. We measured the transmittance T and reflectance R to calculate the normalized absorptance $A = (1-R-T)/(1-R)$. Spectra for un-annealed samples are shown in Fig. 1(a). In agreement with previous work,[11] sub-band gap optical absorptance increases with S concentration, and decreases with increasing annealing temperature, as shown in Fig. 1(b).

XES measurements were performed at the Advanced Light Source, Lawrence Berkeley National Laboratory, using

a)Author to whom correspondence should be addressed. Electronic mail: jts48@cornell.edu.

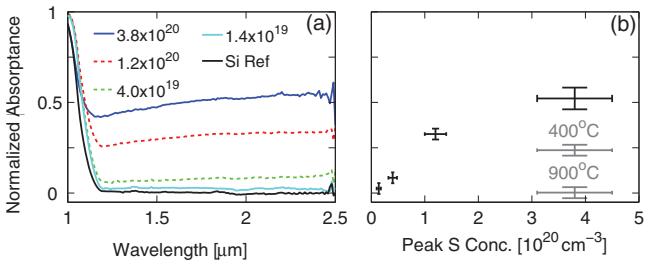

FIG. 1. (Color online) (a) Normalized absorptance spectra for un-annealed samples of different peak S concentrations (cm^{-3}). (b) The average normalized absorptance over the wavelength range 1500-2500 nm plotted vs. peak S concentration for non-annealed samples (black) and two samples annealed at 400 °C and 900 °C, respectively (grey).

the soft x-ray fluorescence spectrometer at Beamline 8.0.1.[12] The energy scale was calibrated by measuring elastically scattered Rayleigh lines at five energies across the measurement window; the excitation energy was calibrated by measuring the x-ray absorption spectrum of a Si reference. The excitation photon energy was 120 eV for all measurements. The integral intensity of all XES spectra are normalized to the spectrum of a reference wafer normalized to unity intensity over the full valence band (VB) emission range (ca. 80–102 eV). A linear background was fit to each spectrum at energies greater than 102 eV and subtracted. The combined attenuation length of the incoming and outgoing photons of the Si $L_{2,3}$ spectra is ca. 30 nm at 45° incidence,[13] and the sulfur concentration only varies by less than 5% over this length scale. The S concentration in the first 45 nm is within the error reported for the peak concentration, located at 100 nm depth.

Fig. 2(a) shows the Si $L_{2,3}$ XES spectra of the Si reference sample and the 3.8×10^{20} cm^{-3} sample. The spectra reveal that S-doping at supersaturated levels does not significantly affect the overall electronic structure (below ca. 99 eV). The emission peaks at ca. 89, 92, and 95 eV are generally attributed to valence bands having a predominantly *s*, *s-p*, and *p* symmetry, respectively.[14] In contrast, the area of the Si $L_{2,3}$ XES marked with a grey dashed box in Fig. 2(a), and magnified in Figs. 2(b) and 2(c), shows the emission originating from states above the VB maximum as a function of S concentration and annealing temperature, respectively. The appearance of two peaks above the VB edge is due to the Si 2p spin-orbit splitting (0.62 eV).[15] The spectra in Fig. 2(b) were measured with a shallower detector angle than those in Fig. 2(c), resulting in an enhanced energy resolution. Thus, an additional spectral structure is resolved (e.g., for the Si reference or the 3.8×10^{20} sample).

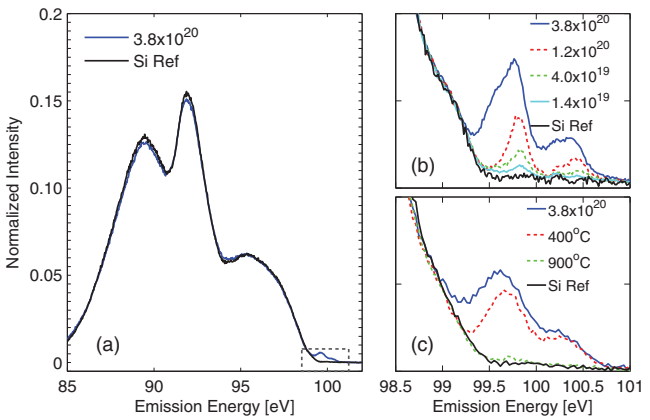

FIG. 2. (Color online) (a) Si $L_{2,3}$ XES spectra of the Si reference and a Si sample doped with S at a peak concentration of 3.8×10^{20} cm^{-3}. Magnified view of the emission seen above the VB maximum for samples of (b) varying concentration (in cm^{-3}) and (c) 3.8×10^{20} cm^{-3} S samples annealed at varying temperatures. Y-axes tick marks denote equal value changes.

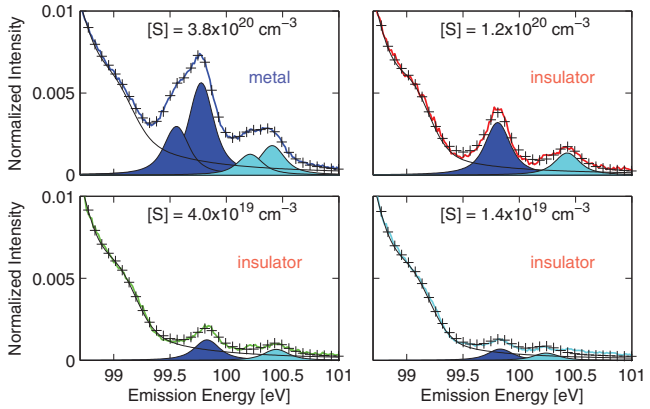

FIG. 3. (Color online) Si $L_{2,3}$ XES spectra from Figure 1(b), along with Voigt-lineshape fits (black crosses). The VB emission fit is shown as a thin black line, and the S-induced emission features are shown as filled light and dark curves, representing L_2 and L_3 contributions, respectively. Peak S concentration is reported in the top right of each graph. The sample with S concentration above the critical insulator-to-metal concentration (see Ref. 7) is labeled "metal," while those below are labeled "insulator."

Using Fityk,[16] Voigt functions were fit to the XES spectra to quantify the independent contributions of the Si VB and the above-edge portions of the spectra, as shown in Fig. 3. Two Voigt functions (centered at 98.3 eV and 99.1 eV) were used to approximate the shape of the VB emission. Pairs of Voigt functions with a constant shape—FWHM of 0.27 eV, spin-orbit splitting of 0.62 eV—were used to approximate the above-VB emission features. Excellent agreement of the fit can be achieved, suggesting that the spectra indeed only require one pair of Voigt peaks for satisfactory description, with the exception of the highest-concentration sample, which clearly requires two pairs of spin-orbit-split Voigt peaks, with the second set centered 0.2 eV below the main peaks.

Fig. 4(a) shows that the area of the above-VB XES features increases linearly with S concentration. This trend indicates that the XES emission features are a result of the

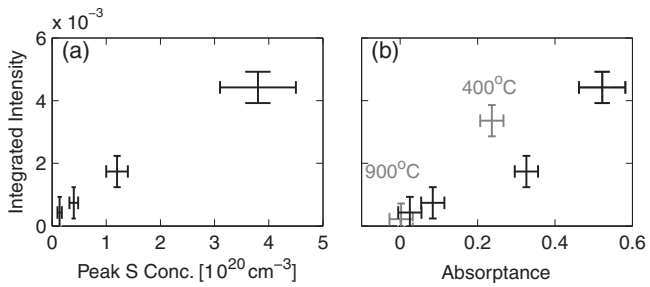

FIG. 4. Area of the above-VB XES emission feature, plotted against (a) peak S concentration for samples of varying dose and (b) average normalized absorptance in the region from 1500 to 2500 nm (black). In (b), grey crosses indicate samples after annealing.

presence of S atoms in the Si samples. Additionally, XES measurements performed on a control sample (PLM-processed Si-implanted Si wafer) produced a spectrum that was indistinguishable from the Si reference; thus, we conclude that the emission features are not related to process-induced defects, but are a result of the S dopants.

As the S concentration surpasses the critical value ($3.1 \pm 1.3 \times 10^{20}$ cm^{-3}) for the insulator-to-metal transition,[7] the shape of the S-induced Si $L_{2,3}$ emission features changes. The spectra in Fig. 3 are labeled "metal" or "insulator" depending on whether their S concentrations lies above or below this critical value,[7] respectively. The insulating samples (1.4×10^{19}, 4.0×10^{19}, and 1.2×10^{20} cm^{-3} peak S concentration) all exhibit an L_3 XES peak centered around 99.7 eV that grows in amplitude, but not in width. However, the expected metallic sample (3.8×10^{20} cm^{-3}) exhibits an XES emission feature with a different spectral shape, and fitting requires a second pair of Voigt functions, as mentioned.

The XES spectral shape change presumably reflects S-induced changes in the ground state electronic structure of Si. One possible explanation is that the delocalization of the S-donor electron ionizes many S dopants. In dilute concentrations, ionized S atoms introduce electronic states farther from the conduction band than those of neutral S (Ref. 3) and may thus result in lower-energy emission when probed via Si $L_{2,3}$ XES. Alternatively, the spectral-shape change could reflect a broader distribution of impurity states: as the inter-atomic distance between S-donors decreases, overlap of the S-donor electron wave functions increases along with the bandwidth of electronic energy levels they introduce. This could lead to a comparable broadening of the XES emission features.

Similar but weak features above the VB edge at similar energy have been observed previously in crystalline Si and were solely attributed to emission from a core-exciton.[17] While aforementioned arguments assert the emission features are tied to the sulfur-induced electronic changes in the material system, the exact excitation-relaxation process is unknown and may be influenced by the presence of excitonic states.

The intensity of the S-induced XES features not only correlates with the sulfur concentration, but also with sub-band gap optical absorption, as shown in Fig. 4(a). Previous work[5] demonstrated that thermal annealing deactivates sub-band gap optical absorption. Fig. 2(c) shows a decrease in S-induced XES emission intensity with increasing annealing temperature, suggesting the features are related to sub-band gap absorptance. In Fig. 4(b), the relationship between absorptance and S-induced XES emission feature area is quantified for un-annealed (black crosses) and annealed (3.8×10^{20} sample, grey crosses) samples. Fig. 4(b) demonstrates that strong sub-band gap absorption correlates with strong above-VB XES emission features, with slight differences between the annealed and un-annealed samples.

Unpublished data indicate that similar anneals do not change the S distribution within the SIMS depth resolution. Thus, the intensity decrease of the S-induced XES feature (Fig. 2(c)) is not due to S evaporation from the surface or diffusion into the substrate. Instead, it suggests an annealing-induced chemical state change of S, which results in an electronic structure change. This is consistent with extended x-ray absorption fine structure studies of chalcogen-doped Si.[18]

In summary, Si $L_{2,3}$ XES spectra of highly S-doped crystalline Si samples, prepared by ion implantation and PLM, exhibit characteristic emission features located above the Si valence band maximum. The emission feature intensities scale linearly with S concentration, indicating that they are induced by the S dopants. More interestingly, the evolution of the XES lineshape shed new light on understanding the insulator-to-metal transition of a deep-level impurity. Additionally, sub-band gap optical absorption correlates with the XES emission feature under varying dopant dose and sample annealing conditions.

This work was supported by the Chesonis Family Foundation, the U.S. Army–ARDEC (Contract No. W15QKN-07-P-0092), the U.S. Army Research Office (Grant No. W911NF-09-1-0470), and the Impuls-und Vernetzungsfonds of the Helmholtz-Association (VH-NG-423). J.T.S. acknowledges a National Science Foundation Graduate Research Fellowship, A.J.S. a Fulbright fellowship, and D.R. a Department of Defense National Defense Science and Engineering Graduate Fellowship. The A.L.S. is funded by the Department of Energy, Basic Energy Sciences (Contract No. DE-AC02-05CH11231).

[1] A. Luque and A. Martí, Phys. Rev. Lett. **78**, 5014 (1997).
[2] A. Luque and A. Martí, Adv. Mater. **22**, 160 (2010).
[3] E. Janzén, R. Stedman, G. Grossmann, and H. G. Grimmeiss, Phys. Rev. B **29**, 1907 (1984).
[4] K. Sánchez, I. Aguilera, P. Palacios, and P. Wahnón, Phys. Rev. B **82**, 165201 (2010).
[5] T. G. Kim, J. M. Warrender, and M. J. Aziz, Appl. Phys. Lett. **88**, 241902 (2006).
[6] C. Wu, C. H. Crouch, L. Zhao, J. E. Carey, R. Younkin, J. A. Levinson, E. Mazur, R. Farrell, P. Gothoskar, and A. Karger, Appl. Phys. Lett. **78**, 1850 (2001).
[7] M. T. Winkler, D. Recht, M. Sher, A. Said, E. Mazur, and M. Aziz, Phys. Rev. Lett. **106**, 178701 (2011).
[8] M. Tabbal, T. Kim, J. M. Warrender, M. J. Aziz, B. L. Cardozo, and R. S. Goldman, J. Vac. Sci. Technol. B **25**, 1847 (2007).
[9] S. H. Pan, D. Recht, S. Charnvanichborikarn, J. S. Williams, and M. J. Aziz, Appl. Phys. Lett. **98**, 121913 (2011).
[10] M. J. Aziz, C. W. White, J. Narayan, and B. Stritzker, in *Energy Beam Solid Interactions and Transient Thermal Processing*, edited by V. T. Nguyen and A. G. Cullis (Editions de Physique, Paris, 1985), p. 231.
[11] B. P. Bob, A. Kohno, S. Charnvanichborikarn, J. M. Warrender, I. Umezu, M. Tabbal, J. S. Williams, and M. J. Aziz, J. Appl. Phys. **107**, 123506 (2010).
[12] J. J. Jia, T. Callcott, J. Yurkas, A. W. Ellis, F. J. Himpsel, M. G. Samant, J. Stöhr, D. L. Ederer, J. A. Carlisle, E. A. Hudson, L. J. Terminello, D. K. Shuh, and R. C. C. Perera, Rev. Sci. Instrum. **66**, 1394 (1995).
[13] B. L. Henke, E. M. Gullikson, and J. C. Davis, At. Data Nucl. Data Tables **54**(2), 181 (1993).
[14] J. E. Rubensson, D. Mueller, R. Shuker, D. L. Ederer, C. H. Zhang, J. Jia, and T. A. Calcott, Phys. Rev. Lett. **64**, 1047 (1990).
[15] L. Ley, J. Reichardt, and R. L. Johnson, Phys. Rev. Lett **49**, 1664 (1982).
[16] M. Wojdyr, J. Appl. Cryst. **43**, 1126 (2010).
[17] R. D. Carson and S. E. Schnatterly, Phys. Rev. Lett. **59**, 319 (1987).
[18] B. K. Newman, J. T. Sullivan, M. T. Winkler, M. J. Sher, M. A. Marcus, S. Fakra, M. J. Smith, S. Gradecak, E. Mazur, and T. Buonassisi, in *Proceedings of the 24th European Photovoltaic Solar Energy Conference, Hamburg, Germany* 2009, p. 236.